sustainability

MDPI

Article

Probabilistic Planning for an Energy Storage System Considering the Uncertainties in Smart Distribution Networks

Ahmed A. Alguhi [1,2,*], Majed A. Alotaibi [1,2] and Essam A. Al-Ammar [1,2]

[1] Electrical Engineering Department, Faculty of Engineering, King Saud University, Riyadh 11421, Saudi Arabia; majedalotaibi@ksu.edu.sa (M.A.A.); essam@ksu.edu.sa (E.A.A.-A.)
[2] K.A.CARE Energy Research and Innovation Center in Riyadh, King Saud University, Riyadh 11421, Saudi Arabia
* Correspondence: 441106438@student.ksu.edu.sa

Abstract: Today, many countries are focused on smart grids due to their positive effects on all sectors of a power system, including those of operators, utilities, and consumers. Furthermore, the usage of renewable energy sources for power production is quickly expanding due to the depletion of fossil fuels and the emissions caused by their use. Additionally, intermittent power generation from renewable energy sources, such as wind and solar, necessitates the use of energy storage devices with which to ensure a continuous power supply to meet demand. This can be accomplished by employing an appropriate storage device with a sufficient storage capacity, thus enabling a grid-connected solar PV and wind system to have enhanced performance and to reduce adverse effects on the power quality of the grid. In this study, a probabilistic planning model that takes the intermittent natures of solar irradiances, wind speeds, and system demands into account is introduced. A novel criterion is also adopted to map the three-dimensional spaces of intermittency with the proposed model for optimizing BESS charging/discharging decisions. This planning model is intended to minimize the economic costs of investment and operation of a battery energy storage system (BESS) for a planning period. Moreover, the substation and feeder upgrade costs, as well as the overall system loss costs, are included in the proposed model. Particle swarm optimization (PSO) is utilized to find the optimal sizing, location, and operation of energy storage systems. The proposed methodology was validated using a 69-bus distribution system.

Keywords: BESS; PV-based DG; wind-based DG; power system planning; smart distribution network; PSO

Citation: Alguhi, A.A.; Alotaibi, M.A.; Al-Ammar, E.A. Probabilistic Planning for an Energy Storage System Considering the Uncertainties in Smart Distribution Networks. *Sustainability* **2024**, *16*, 290. https://doi.org/10.3390/su16010290

Academic Editor: Bowen Zhou

Received: 18 October 2023
Revised: 27 November 2023
Accepted: 11 December 2023
Published: 28 December 2023

1. Introduction

Electricity distribution networks hold a pivotal position within power delivery systems, which is primarily because of their proximity to end users. Over the last few years, distribution networks have witnessed the integration of numerous innovative technologies in response to various technical and economic factors. Among these advancements, energy storage systems (ESSs) have emerged as a technology poised to assume a vital role in the energy sector's imminent future. ESSs are anticipated to deliver electricity with the utmost cost efficiency and the requisite level of quality [1].

ESSs come in various forms, from traditional batteries to cutting-edge technologies, such as pumped hydro energy storage and thermal energy storage. The planning, deployment, and management of these systems are at the heart of the energy transition, enabling us to harness the full potential of renewable resources and enhance grid resilience.

The challenges of ESS planning are formidable but surmountable. Energy storage planning requires interdisciplinary collaboration among engineers, policymakers, economists, and environmentalists. It demands a holistic approach that considers not only technical feasibility but also the socioeconomic and environmental impacts of energy storage

projects. It necessitates innovation in policy frameworks, market structures, and regulatory mechanisms to incentivize investments in energy storage infrastructure.

Saudi Arabia has taken significant measures to incorporate renewable energy sources—alongside its traditional reliance on oil and gas—within the national energy blend. Saudi Vision 2030 lays out a strategic plan for the nation to reduce its dependence on oil in the energy mix, acknowledging that Saudi Arabia is currently progressing in the development of a competitive renewable energy sector. One of the main forces behind sustainability is the development of renewable energy projects, which will help reduce emissions and replace high-value fuel in power production. Indeed, energy storage can help address the problems with renewable energy, such as intermittent solar and wind output power levels.

ESSs possess the ability to swiftly address substantial shifts in energy demand, enhancing grid responsiveness, minimizing the necessity for constructing backup power facilities, and effectively mitigating the intermittency challenges associated with solar and wind energy generation. However, incorporating ESSs in a distribution system without optimizing their size, location, and operation mechanisms will affect the stability and dependability of the power system. Therefore, optimizing the allocation and capacity of ESSs within a network is essential for enhancing their performance and improving the overall performance and quality of a power system.

The selection of an ESS is dependent on the application of its use. For example, suppose that it is used to supply power during transitions between power sources. In that case, one should select either capacitor storage or an SMES; however, when it is used for power quality applications, one should choose an ESS such as a PHS, flywheel, SMES, CAES, or capacitor. Further, if energy management is the desired application, a battery energy storage system (BESS) is the most proper choice of ESS; therefore, in this study, a BESS was chosen as the candidate ESS in the application under study since its rated power and discharge time were suitable for the application of interest [2].

Based on a survey of the literature, the following referenced articles contributed to the understanding and advancement of BESSs from various perspectives. Ref. [3] presented a comprehensive review encompassing BESS technologies, optimization objectives, constraints, approaches, and outstanding issues, providing a broad overview of the current landscape. Ref. [4] focused on the specific context of New York State while investigating the impacts of BESS technologies and the integration of renewable energy on the energy transition, offering insights into regional dynamics. Ref. [5] presented a modeling approach for a large-scale BESS and emphasized its application to power grid analysis. Ref. [6] contributed to the integration of BESSs into multi-megawatt grid-connected photovoltaic systems and addressed the complexities of large-scale renewable integration. Ref. [7] offered a methodological framework for site selection and capacity setting for BESSs in distribution networks with renewable sources, contributing practical strategies for optimal deployment. Additionally, there has been much research providing comprehensive overviews of ESSs in distribution networks with a focus on placement, sizing, operation, and power quality to enhance the performance and reliability of distribution networks. Ref. [8] offered an extensive overview that covered various aspects of ESSs in distribution networks. Ref. [9] contributed insights into the optimal location, selection, and operation of BESSs and renewable distributed generation in medium–low-voltage distribution networks. Ref. [10] presented an approach based on genetic algorithms for the integration of energy storage systems in AC distribution networks that addressed their optimal location, selection, and operation. Ref. [11] focused on low-voltage residential networks in the UK while addressing the optimal placement, sizing, and dispatch of multiple BESSs. Ref. [12] introduced a PSO algorithm for optimizing energy storage capacities in distribution networks while considering probability correlations between wind farms. Ref. [13] investigated the installation of battery energy storage systems with renewable energy resources in distribution systems while considering various load models. Ref. [14] discussed energy storage optimization in the configuration of active distribution networks using distributed approaches. Ref. [15] explored the optimal allocation and operation of an energy storage

system with high-penetration grid-connected photovoltaic systems, contributing to the sustainable integration of renewable energy in distribution networks. Ref. [16] introduced the Whale Optimization Algorithm for optimizing the placement and sizing of BESSs to reduce losses, contributing to efficiency improvements in distribution networks. Ref. [17] focused on energy storage system scheduling for peak demand reduction by employing evolutionary combinatorial optimization techniques to enhance sustainable energy technologies. Ref. [18] addressed distributed generation and energy storage system planning for a distribution system operator and highlighted the importance of integrated planning for improving system efficiency. Refs. [19,20] contributed to optimal ESS allocation for benefit maximization and load shedding to improve the reliability of distribution systems and employed advanced optimization techniques, respectively. Ref. [21] provided an economic analysis model for an ESS applied to a distribution substation and offered insights into the economic feasibility of ESS integration. Ref. [22] conducted an analysis of the adequacy and economics of distribution systems integrated with electric energy storage and renewable energy resources, and they emphasized the importance of considering both adequacy and economic aspects in system planning.

Even though numerous studies have explored various optimization methods for energy storage technologies (ESTs), there is a noticeable scarcity of comprehensive information and up-to-date data pertaining to the comprehensive planning and application potential of ESSs for the integration of renewable energy sources (RESs) into distribution planning. In addition, in response to the escalating energy demand, the heightened integration of renewable sources, and the recent evolution of grid demand, there is a critical need for comprehensive energy storage planning strategies. Additionally, there is a pressing need for further research that assesses the impacts of ESSs on distribution systems while considering both technical and economic constraints. Thus, this study aims to bridge this knowledge gap by investigating the optimization of energy storage within distribution systems that incorporate renewable energy sources, such as DGs, and a novel criterion for mapping the three-dimensional spaces of intermittency with the proposed model is adopted to optimize BESS charging/discharging decisions. The objective is to minimize the total planning and operational costs while considering technical and economic constraints and, ultimately, identifying the most cost-effective solutions for the placement and sizing of energy storage units within a smart distribution network.

The main contributions of this study are the following.

1. A robust probabilistic planning model for BESSs in distribution networks is developed in order to optimize the location, sizing, and operation of BESSs and to determine the most economical BESS with the lowest overall planning cost while taking uncertainties in wind speed, solar irradiance, and system demand into account and considering technical and economic factors.
2. The proposed model brings a significant advantage for distribution companies, as it strategically addresses challenges such as energy losses, deferral of system upgrades, and effective energy management during off-peak and on-peak periods. By maximizing benefits through these considerations, the model contributes to the overall efficiency and sustainability of distribution networks.
3. In contrast to previous approaches that focused solely on the demand state for charging and discharging BESSs, this study introduces a novel paradigm. It employs three-dimensional spaces encompassing the wind state, PV state, and demand state to optimize charging and discharge decisions. By evaluating the interplay of these dimensions, the optimization model makes informed decisions regarding energy production or absorption, ultimately minimizing the planning and operational costs for the entire system.
4. This research makes a valuable contribution to the electricity sector by providing an opportunity for electricity utilities to leverage the study's findings to advance the transition toward renewable energy sources.

5. This study's findings can be leveraged to advance the transition toward sustainability in the energy sector.

2. Modeling of Uncertainties

The uncertainty in smart distribution networks is a critical area of research and development in the field of electrical power systems. As the integration of renewable energy sources, advanced monitoring and control technologies, and the increasing complexity of grid operation become more prevalent, it is essential to have a robust theoretical foundation for dealing with uncertainty. In this context, uncertainty refers to the variations and unpredictability in generation, consumption, and grid conditions that can affect the safe and efficient operation of an electrical grid.

The most significant theoretical enhancements and considerations related to the description of uncertainty in a smart distribution network are as follows.

1. Stochastic models: Traditional deterministic models of power system operation are no longer sufficient to capture the complexity of modern distribution networks. Stochastic models, which incorporate probability distributions for various parameters, are gaining importance. These models allow for a more realistic representation of uncertainties, such as the intermittent nature of renewable energy generation or the variability in electricity demand.
2. Incorporating renewable energy sources: With the increasing penetration of renewable energy sources, such as wind and solar, uncertainty in generation becomes a significant concern. Theoretical improvements involve better modeling of the variability and intermittency of renewable generation, as well as their spatial and temporal correlations. This can be achieved through advanced statistical methods, such as time-series analysis and probabilistic forecasting techniques.
3. Demand uncertainty: Electricity demand can also be uncertain due to factors such as weather conditions, economic fluctuations, and changes in consumer behavior. Theoretical improvements should focus on capturing this demand uncertainty, including short-term load forecasting and the development of probabilistic demand models.

Therefore, the location of renewable resources in a distribution system requires effective modeling of demand and DGs. In some research, such as that in Ref. [13], the authors used deterministic methods that represented the demand and DGs as constant power based on their average or maximum power; although these methods can be easily executed, they may lead to unrealistic and inaccurate results. Therefore, much research considered the stochastic nature of demand and renewable resources to find more accurate and realistic results. This stochastic nature can be taken into account by using either time-series modeling or probabilistic modeling, which are the two main methods for modeling the nature of such systems [18–20,23–25]. However, in a recent lecture [26], the methodologies employed for modeling the nature of systems were thoroughly examined in order to move beyond conventional time-series and probabilistic approaches. The lecture spotlighted alternative techniques, such as robust optimization, information gap decision theory (IGDT), and interval approaches, among others, offering a mosaic of tools for researchers. The selection of a specific method depends on the nature of the system, the type of data available, and the goals of the analysis.

Much research, such as that in Ref. [18], has used the time series to model the stochastic nature of system components; this approach proposes a forecasting horizon of one year ahead for both demand and renewable resources. Then, it uses the forecasted shape to determine an ESS's charging and discharging power at each hour. This is hard to implement for a year-long planning model, and it requires a very long time for the simulation for vast sets of historical data. This may lead to unrealistic and inaccurate results. Therefore, probabilistic methods are effective for year-long planning models, as they can handle the stochastic nature of demand, wind speed, and solar irradiance, as described in [19,20,23–25]. This is because they can be easily implemented and require less time for simulations with vast sets of historical data in comparison with time-series models. A probabilistic model

was applied in this study to model the stochastic nature of wind speed, solar irradiance, and demand fluctuation. In this method, historical data on the wind speed, solar irradiance, and demand fluctuation were described by using a specific probability distribution function (PDF) (1). Then, this PDF was divided into several states, which were used to generate a probabilistic model for the load, wind speed, and solar irradiance.

The wind speed, solar irradiance, and load are assumed to be independent in this work.

$$p(x) = P[a < x \leq b] = \int_a^b f(x).dx \tag{1}$$

These were modeled as described in the following.

2.1. Modeling of the Wind Speed and Wind Turbine Output Power

In this study, we opted for the Weibull distribution to capture the intermittent nature of wind speed data, a choice that is commonly employed in numerous studies [23,24]. We developed a probabilistic wind speed model with a step size of 1.1 m/s. For any given wind speed dataset, it is crucial to ascertain the mean (μ) and the standard deviation (σ) of the data. Additionally, the wind speed characteristics at any location are characterized by the Weibull scale parameter (c) and the Weibull shape parameter (k). The key parameters of a wind turbine include the cut-in speed (v_{in}), rated speed (v_r), cut-out speed (v_{out}), and rated or maximum output power (P_{wr}). Equation (2) defines the Weibull distribution function, while Equation (3) is used to compute the Weibull distribution parameters [24].

$$f(v) = \frac{k}{c}\left(\frac{v}{c}\right)^{k-1} exp\left[-\left(\frac{v}{c}\right)^{k}\right] \tag{2}$$

$$k = \left(\frac{\sigma}{\mu}\right)^{-1.086}, c = \frac{\mu}{\Gamma\left(1+\frac{1}{k}\right)} \tag{3}$$

As can be seen in Figure 1, the characteristic curve of wind power can be categorized into three distinct regions: no wind power, de-rated power, and rated power. The area in which there is no wind power is defined as the area in which the wind speed is less than the turbine's cut-off speed. The turbine's blades are unable to overcome the friction generated prior to a speed reduction because there is not enough torque. In the de-rated speed region, the output power of the turbine dramatically increases to achieve the rated power of the turbine as the wind speed rises over the cut-off speed. In the rated power region, the wind speed exceeds the turbine's cut-out speed, and the wind turbine will shut down as a preventative measure to protect the rotor from the strong forces acting on the turbine's structure. A wind turbine's output power can be obtained from (4) [23,24]. Table 1 provides the data parameters for the wind turbine and required wind speed in this study, while Table 2 presents the multistate probability model of a wind-based DG.

$$P_w(v) = \begin{cases} 0, & 0 < v < v_{in} \ \ and \ v > v_{out} \\ P_{wr}\left(\frac{v-v_{in}}{v_r-v_{in}}\right), & v_{in} < v < v_r \\ P_{wr} & v_r < v < v_r \end{cases} \tag{4}$$

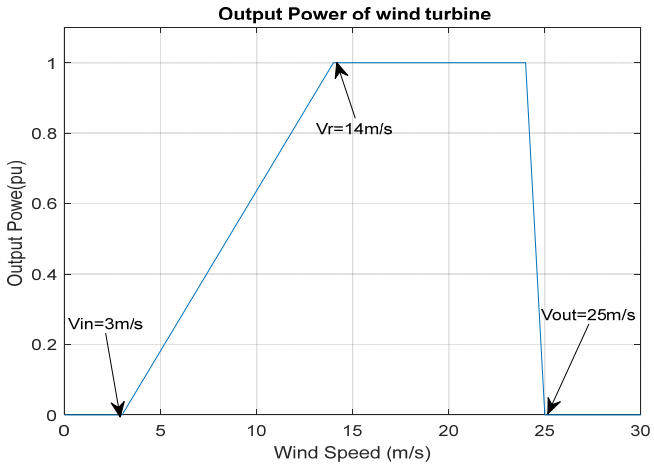

Figure 1. Power characteristic curve of a wind turbine.

Table 1. Wind speed and wind turbine parameters.

Parameters	Value
Rated power (P_r)	1000 kW
Cut-in speed (v_{in}) m/s	3
Rated speed (v_r) m/s	14
Cut-out speed (v_{out}) m/s	25
Weibull scale parameter c	4.2483
Weibull shape parameter k	1.6515

Table 2. Multi-state probability model of a wind-based DG.

State	Lower (m/s)	Upper (m/s)	% Output Power	Probability
1	0	3 and >25	0	0.4305
2	3	4.1	5	0.18007
3	4.1	5.2	15	0.14195
4	5.2	6.3	25	0.10046
5	6.3	7.4	35	0.06501
6	7.4	8.5	45	0.0389
7	8.5	9.6	55	0.0217
8	9.6	10.7	65	0.01134
9	10.7	11.8	75	0.00558
10	11.8	12.9	85	0.00259
11	12.9	14	95	0.00114
12	14	25	100	0.000772

2.2. Solar Irradiance and PV Output Power Models

Similar to when modeling the wind speed, there are various distributions available for studying the uncertainty associated with solar irradiance based on its statistical properties. The probability density function that mirrors the probabilistic behavior of solar irradiance (s) can be represented by using the Beta probability density function $f(s)$, as outlined in Equation (5). The calculation of the Beta distribution parameters β and α is demonstrated in Equation (6) [23,24]. Table 3 provides the data parameters of the solar system needed in this study.

$$f(s) = \begin{cases} \frac{\Gamma(\alpha+\beta)}{\Gamma(\alpha)\,\Gamma(\beta)} s^{(\alpha-1)}(1-s)^{(\beta-1)}, & 0 \le s \le 1 \\ 0 \;\; o.w \end{cases} \tag{5}$$

$$\beta = \frac{(1-\mu)\sigma^2}{\mu(1-\mu)-\sigma^2} \quad \text{and} \quad \alpha = \frac{\beta \times \mu}{(1-\mu)} \tag{6}$$

Table 3. Solar irradiance and PV parameters.

Parameters	Value
Rated PV power (P_{PVr})	500 kW
Adjustable value of irradiance r_C	200 W/m^2
Standard irradiance s_{STD}	1000 W/m^2
Beta parameter β	0.45
Beta parameter α	1.438

The level of PV generation power is intricately linked to the solar irradiance. Consequently, the PV output power can be obtained by using Equation (7) [27]. Table 4 presents the multi-state probability model of a PV-based DG.

$$P_{PV}(s) = \begin{cases} P_{PVr}\left(\frac{s^2}{s_{STD} \times r_C}\right) \; for \; 0 < s < r_C \\ P_{PVr}\left(\frac{s}{s_{STD}}\right) \; for \; r_C \leq s < s_{STD} \\ P_{PVr} \; for \; s > s_{STD} \end{cases} \quad (7)$$

Table 4. Multi-state probability model of a PV-based DG.

State	Lower (kW/m^2)	Upper (kW/m^2)	% Output Power	Probability
1	0	0.084	0	0.395786
2	0.084	0.168	7.94	0.138345
3	0.168	0.252	21	0.098823
4	0.252	0.334	29.3	0.076266
5	0.334	0.418	37.6	0.064414
6	0.418	0.502	46	0.054077
7	0.502	0.586	54.4	0.045772
8	0.586	0.67	62.8	0.03867
9	0.67	0.754	71.2	0.032253
10	0.754	0.838	79.6	0.026061
11	0.838	0.922	88	0.019489
12	0.922	1	96.1	0.010005

2.3. Demand Models

The normal distribution function ($f(d)$), as outlined in Equation (8), was employed to serve as a probabilistic model for representing the system demand behavior, a choice aligned with prior studies [23,24]. The analysis encompassed 8760 hours of load data points—specifically, those of the IEEE's Reliability Test System (RTS)—with a mean of μ = 0.6142 and a standard deviation of σ = 0.1448. Table 5 illustrates the multi-state probability model for demand.

$$f(d) = \frac{1}{\sigma\sqrt{2\pi}} e^{-\frac{1}{2}\left(\frac{d-\mu}{\sigma}\right)^2} \quad (8)$$

Table 5. Multi-state probability model of demand.

State	Lower Load (pu)	Upper Load (pu)	Probability
1	0	0.35	0.03402
2	0.35	0.41	0.045205
3	0.41	0.47	0.08042
4	0.47	0.53	0.1208
5	0.53	0.59	0.1532
6	0.59	0.65	0.164
7	0.65	0.71	0.14825
8	0.71	0.77	0.1131
9	0.77	0.83	0.0729
10	0.83	0.89	0.0397
11	0.89	0.95	0.01821
12	0.95	1	0.00634

2.4. Generating Operating Scenarios for the Overall System

After establishing the probability distribution functions for the wind speed, solar irradiance, and system demand, the next step involved partitioning these PDFs into numerous discrete states for their integration into the calculations. The process of selecting these states carried significant importance, as it entailed striking a delicate balance between the precision of the outcomes and the intricacy of the analysis. The division of the PDFs into multiple equidistant intervals depended on factors such as the maximum value and the number of intervals necessary, as shown in Ref. [25].

Once all of the states for the wind power, solar power, and system load were defined, a three-column matrix encompassing every conceivable combination of these states—or scenario—was constructed. In this matrix, the first column signified the various levels of load states, the second column represented the states of the solar DG output power, and the third column signified the wind-based DG output, as shown in Table 6. This multi-scenario matrix was structured with a number of rows equal to the total number of scenarios, which was determined by multiplying the numbers of wind states, solar states, and load states. The probability associated with each scenario was calculated as the product of the probabilities of the wind state, solar state, and load state for that specific scenario, assuming that the wind speed, solar irradiance, and load were independent events.

Table 6. The column matrix for all possible scenarios for all states.

Scenarios	Demand Power (P_L)	PV Power (P_{PV})	Wind Power (P_w)
1	L	L	L
2	L	L	H
3	L	H	L
-	-	-	-
-	-	-	-
-	-	-	-
-	-	-	-
-	-	-	-
-	-	-	-
-	-	-	-
-	-	-	-
N	H	H	H

L represents a lower-power state and H represents a higher-power state; N = 12 × 12 × 12.

3. Problem Formulation and Planning Model

This section outlines the formulation of the problem of the proposed probabilistic planning model for a BESS and explains how BESSs can be integrated into power distribution networks alongside renewable energy resources. The probabilistic planning model encompassed the modeling of probabilistic PV and wind power outputs, as well as the probabilistic representation of system demand. Within this model, various factors were considered, including the costs associated with investment in and operation of BESSs, substation and transmission line upgrades, and power losses. The primary objective of this planning was to minimize the cumulative investment and operational costs over the planning horizon, and this optimization was achieved by determining the optimal placement, sizing, and operation of BESSs.

3.1. Objective Function

The objective function is composed of BESS investment costs (BC_i) and economic costs of operation (BC_{eop}), along with substation and feeder costs (SC_{su}) and power loss costs (LC_L). Equation (9) presents the mathematical representation of this objective function.

$$\text{Min} \sum \text{cost} = min\left(NPV\left(BC_{in} + BC_{eop} + SC_{su} + LC_{Line}\right)\right) \quad (9)$$

The mathematical formulations for each term in the objective function are displayed in Equations (10) through (13). The net present value (*NPV*) can be computed either from the future value (*FV*), as expressed in Equation (14), or from the annual value (*AV*), as described in Equation (15).

$$BC_{in} = \sum_{i=1}^{N}\Big(C_p \times P_{BESS,N}^{rated} + C_E \times E_{BESS,N}^{rated}\Big) \tag{10}$$

$$\begin{aligned} BC_{eop_{yr}} = \sum_{\xi}((&8760 \times p(\xi_{ch}) \times C_{price\_off} \times P_{yr,\xi_{ch}}^{ch}) \\ &- \Big(8760 \times p(\xi_{dis}) \times C_{price\_on} \times P_{yr,\xi_{dis}}^{dis}\Big)), \forall yr \end{aligned} \tag{11}$$

$$\begin{aligned} LC_{Line_{yr}} = \sum_{\xi}((&C_{\,price\_off} \times 8760 \times p(\xi_{ch}) \times \sum_{ij=1}^{N_{line}} P_{ij,\ yr,\xi_{ch,}}^{loss}) \\ &+ (C_{\,price\_on} \times 8760 \times p(\xi_{dis}) \times \sum_{ij=1}^{N_{line}} P_{ij,\ yr,\xi_{dis,}}^{loss})), \forall yr \end{aligned} \tag{12}$$

$$SC_{su_{yr}} = Transmission\ cost + substation\ cost \tag{13}$$

$$NPV = \frac{FV}{(1+IR)^n} \tag{14}$$

$$NPV = AV\frac{(1+IR)^n - 1}{IR(1+IR)^n} \tag{15}$$

where C_p is the BESS's power cost in \$/kW, C_E is the BESS's energy cost in \$/kWh, $P_{BESS,N}^{rated}$ is the BESS's rated power at bus number N, $E_{BESS,N}^{rated}$ is the BESS's rated energy at bus number N, ξ_{ch} and $\xi_{dis,}$ are the charging and discharging states, $p(\xi)$ is the probability of each state ξ, C_{price_off} is the energy price at off-peak hours, C_{price_on} is the energy price during peak hours, and $P_{yr,\xi_{ch}}^{ch}$ and $P_{yr,\xi_{dis}}^{dis}$ are the charging and discharging of power at state ξ in year y, respectively. $P_{ij,yr,\xi_{ch,}}^{loss}$ is the power loss of line ij at state ξ, $P_{ij,yr,\xi_{dis,}}^{loss}$ is the power loss of line ij at state ξ in year yr, IR is the interest rate, and n represents the number of years.

3.2. Model Constraints

3.2.1. Network Constraints

Equations (16) and (17) define the power-flow equation during the charging and discharging of the BESS at each bus *i* and state ξ. Equation (18) is used to calculate the reactive power at each bus *i* and state ξ.

$$\begin{aligned} P_{G_{i,\xi,yr}} + C_{w_\xi} \times P_{\,wr_i} + C_{PV_\xi} \times P_{\,PVr_i} - P_{D\ i,\xi,yr} - \eta_{ch} \times P_{BESS_{\xi,yr}}^{ch} = \textstyle\sum_{j=1}^{N} V_{i,\xi,yr} \times V_{j,\xi,yr} \times Y_{ij} \times \\ \cos(\theta_{ij} + \delta_{j,\xi,yr} - \delta_{i,\xi,yr}), \forall i, \xi \in \xi_{ch,}\ yr \end{aligned} \tag{16}$$

$$\begin{aligned} P_{G_{i,\xi,yr}} + C_{w_\xi} \times P_{\,wr_i} + C_{PV_\xi} \times P_{\,PVr_i} - P_{D\ i,\xi,yr} - \eta_{di\xi} \times P_{BESS_{\xi,yr}}^{dis} = \textstyle\sum_{j=1}^{N} V_{i,\xi,yr} \times V_{j,\xi,yr} \times Y_{ij} \times \\ cos\big(\theta_{ij} + \delta_{j,\xi,yr} - \delta_{i,\xi,yr}\big), \forall i, \xi \in \xi_{dis,}\ yr \end{aligned} \tag{17}$$

$$Q_{G_{i,\xi,yr}} - Q_{D\ i,\xi,yr} = -\textstyle\sum_{j=1}^{N} V_{i,\xi,yr} \times V_{j,\xi,yr} \times Y_{ij} \times sin\big(\theta_{ij} + \delta_{j,\xi,yr} - \delta_{i,\xi,yr}\big),\ \forall i, \xi, yr \tag{18}$$

where $P_{G_{i,,\xi,yr}}$ is the generated power at bus i in state ξ during year yr, $P_{D_{i,\xi,yr}}$ is the demand power at bus *i* in state ξ during year yr, P_{wr} is the rated power of the wind turbine, C_{w_ξ} is the percentage of output power of wind in each state, P_{PVr} is the rated power of the PV unit, C_{PV_ξ} is the percentage of the PV output power in each state, η_{ch} and $\eta_{di\xi}$ are the

charging and discharging efficiency of the BESS, $(V_{i,\xi,yr})$ is the defined voltage at bus i in state ξ in year yr, (Y_{ij}) defines the magnitude of admittances of the line between buses i and j, θ_{ij} is the angle of admittances, and δ is the voltage angle.

Equation (19) is used to calculate the total power loss in the line in state ξ during year yr, and Equation (20) defines the line current between bus i and bus j in state ξ during year yr. Equations (21) and (22) define the per-unit limit of voltage $(V_{i,\xi yr})$ at bus i in state ξ during year yr and the slake voltage $(V_{i,\xi,\mathrm{yr}})$ in state ξ during year yr, respectively. Equation (23) constrains the feeder capacity limit, where $I_{ij,max}$ is the maximum permissible current in the feeder between i and j.

$$P_{\xi,yr}^{loss} = \sum_{j=1}^{N} I_{ij,\xi,yr}^{2} R(ij), \forall i, \xi, yr \tag{19}$$

$$I_{ij,\xi,yr} = \left(\frac{P_{j,\xi,yr} + jQ_{j,\xi,yr}}{V_{j,\xi,yr}} \right)^{*}, \forall i, \xi, yr \tag{20}$$

$$V_{min} \leq V_{i,\xi,yr} \leq V_{max}, \forall i, \xi, yr \tag{21}$$

$$V_{\xi,1,yr} = 1, \ \delta_{\xi,1,yr} = 0, \ \forall \xi, yr \tag{22}$$

$$0 \leq I_{ij,\xi,yr} \leq I_{ijmax} \forall \xi, yr \tag{23}$$

3.2.2. DG Constraints

Equations (24)–(26) constrain the output power of the DG between zero and the rated power.

$$(P\_DG)^2 + (Q\_DG)^2 \leq (S\_DG\_rated)^2 \tag{24}$$

$$0 \leq P\_DG \leq P\_DG\_rated \tag{25}$$

$$0 \leq Q\_DG \leq Q\_DG\_rated \tag{26}$$

3.2.3. BESS Constraints

Equations (27) and (28) define the charging and discharging power of the BESS and constrain its rated power.

$$P_{BESS}^{ch} = \begin{cases} P_{BESS}^{rated}, & P_{BESS}^{ch} \geq P_{BESS\_ch}^{rated} \\ P_{BESS}^{ch}, & P_{BESS\_ch}^{rated} \geq P_{BESS}^{ch} \geq 0 \end{cases} \tag{27}$$

$$P_{BESS}^{dis} = \begin{cases} -P_{BESS}^{dis}, & 0 \geq P_{BESS}^{dis} \geq -P_{BESS\_dis}^{rated} \\ -P_{BESS}^{rated}, & -P_{BESS\_dis\_Max} \geq P_{BESS}^{dis} \end{cases} \tag{28}$$

where P_{BESS}^{ch} is the charging power, P_{BESS}^{rated} is the rated charging power, P_{BESS}^{dis} is the discharging power of the *BESS*, and P_{BESS}^{rated} is the rated discharging power of the *BESS*.

3.3. Algorithm for Solving the Proposed Planning Model

In this study, the particle swarm optimization (PSO) algorithm was utilized to solve the optimization model, as it is gaining recognition as an efficient technique for solving this type of optimization problem. Probabilistic models of the demand, wind-based DG units, PV-based DG units, load growth, system topology, energy price, system data, planning period, discount rate, BESS data, and BESS costs were the main methodology's inputs, and the main outputs of the optimization were the optimal size and location of the BESS units and the BESS units' optimized operation. The proposed methodology's justification was the optimization of the planning costs for distribution utilities through the deployment and management of BESSs. In the process, as shown in Figure 2, before the simulation started, a matrix consisting of the magnitude and the corresponding probability of each state of

the load, wind turbines, and PV units was defined (this represented all of the operating scenarios); then, all required data of the system under study and the PSO algorithm were input to start the simulation. First, the simulation began with the first year to optimize the location, operation, and sizing of the BESSs, and this was controlled by all states of the load, wind, and PV. Secondly, a load flow analysis was performed to calculate the overall system losses and determine the required system upgrades. Finally, the total NPV of the planning was computed, and the most economical solution for PSO was obtained. Then, the algorithm moved to the next year; the load was increased by 5%, and the simulation was performed again until the final planning year was computed. After that, the particle velocity and position in the PSO algorithm were updated, and all steps were repeated until the simulation's termination criteria were fulfilled; then, the final output results were obtained. Table 7 shows a comparison of our proposed model featuring a three-dimensional ESS dispatch with the probabilistic model outlined in Refs. [19,20], which was designed for a load-based ESS dispatch. This comparison took place for the scenario of a lithium-ion PV-based DG, and key performance metrics were assessed. Our model exhibited superior accuracy, resulting in a reduced total cost of 2.451 M$ in comparison with the load-based ESS dispatch probabilistic model's 3.08 M$. Despite the high complexity introduced by our three-dimensional ESS dispatch strategy, our model demonstrated competitive computational efficiency, as it completed the analysis in about 2.5 h, whereas the previous probabilistic model required approximately 2 h. These findings underscore the advancements of our proposed model, which offers improved accuracy and complexity without compromising computational efficiency.

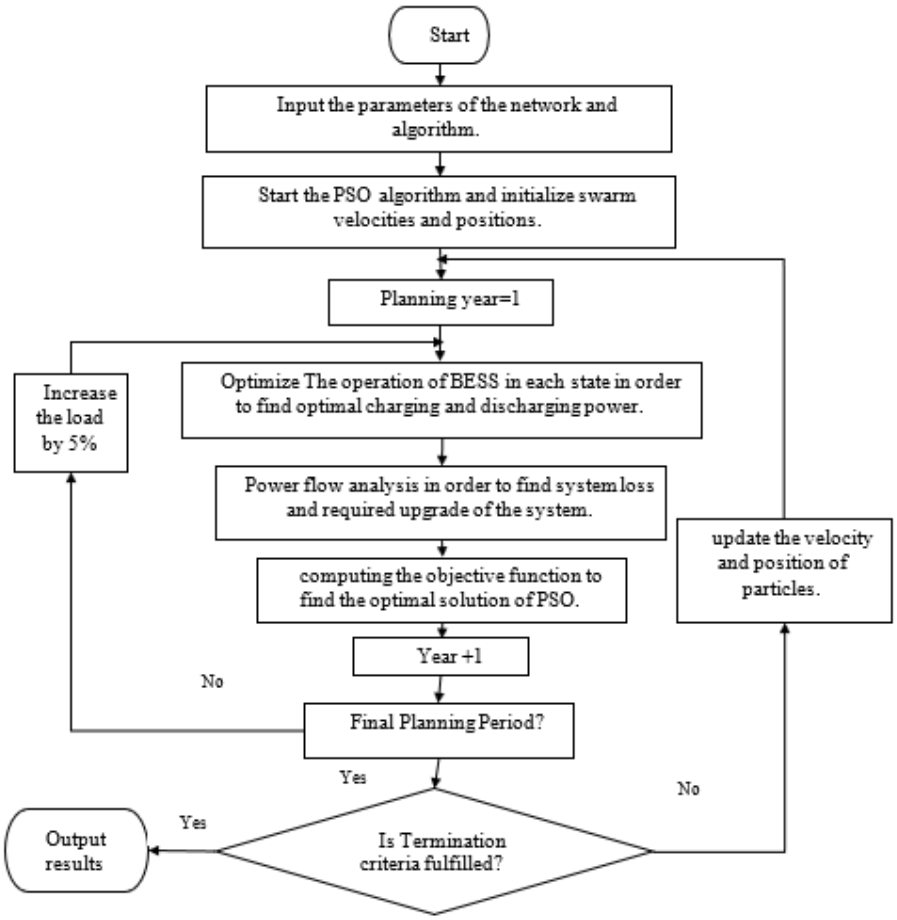

Figure 2. Flowchart of the proposed method.

Table 7. Comparison of our proposed model with an existing model from the literature.

Proposed Model	Objective Function For Lithium-Ion Scenario	Accuracy	Complexity	Computation Time
Probabilistic [19,20] (load-based ESS dispatch)	3.08 M$	High	Moderated	About 2 h
Our proposed model (three-dimensional ESS dispatch)	2.451 M$	Very High	Relatively High	About 2.5 h

4. Case Studies and Results

4.1. The Network System under Study

The proposed planning model was evaluated by using the IEEE69 radial-distribution system, as shown in Figure 3, and its data can be found in [28]. The total system load was 3.802 MW and 2.7 MVAR, with base values of 12.66 KV and 100 MVA [29]. The planning period spanned 15 years, as proposed in this study, with an assumed annual load growth rate of 5%. The costs for off-peak and on-peak power were considered to be $23.6/MWh and $32.5/MWh, respectively [24]. The fixed and variable transmission line costs were assumed to be $150,000/km and $1000/MW, respectively. Furthermore, the fixed and variable substation costs were estimated to be $200,000 and $50,000/MW, respectively [30]. An interest rate of 10% was assumed, and the system operated with a power factor of 0.9.

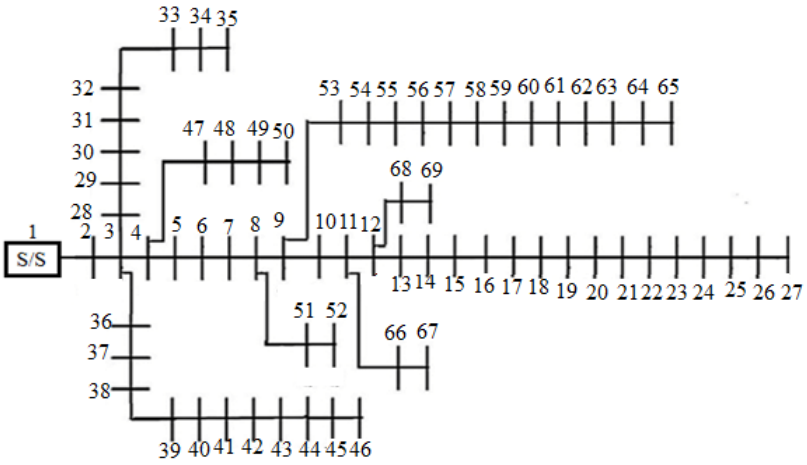

Figure 3. The IEEE69 distribution system.

Two renewable resources were used in this study as DGs: PV and wind-based DGs. The choice of DG power capacity was contingent on the capacity factor of each DG, and DGs with higher capacity factors possessed greater power ratings; in addition, the rating of DG power and the location of DGs in the system in this study depended on the fluctuations in the voltage profile and power loss of the system. Therefore, the sizing and placement of DGs were determined after studying the impacts of different locations and sizes on the voltage profiles and power losses of the system under study. The optimal size for the wind-based DG was determined to be 1 MW when connected to bus #61, while the optimal size for the PV-based DG was found to be 0.5 MW when connected to bus #17. It is noteworthy that the wind-based DG possessed a higher capacity than that of the PV-based DG, which was primarily due to its large capacity factor derived from the wind speed and solar irradiance data utilized in this study. Figures 4–6 depict the voltage profiles, line currents, and active power losses of the system when different types of DGs operated at their rated capacities within the system.

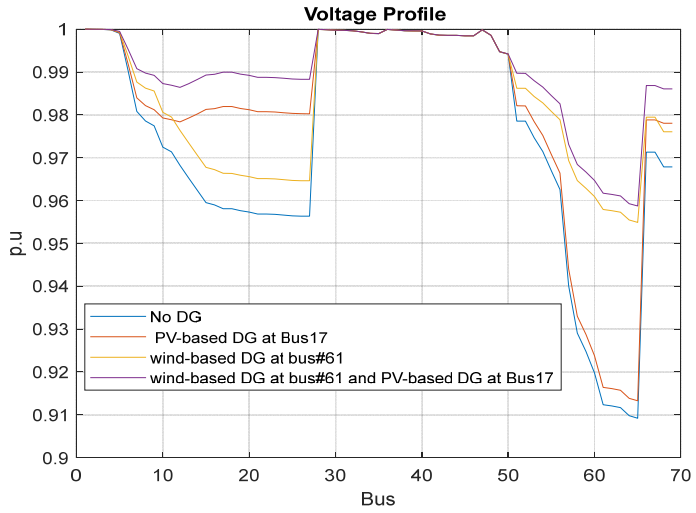

Figure 4. The voltage profiles for different DGs.

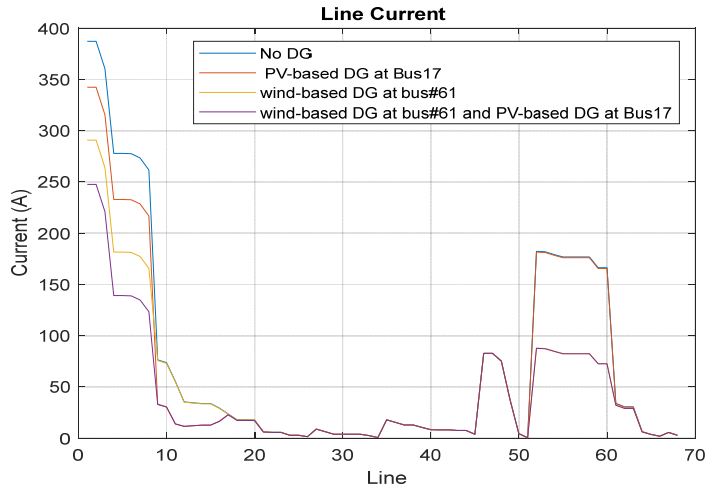

Figure 5. Line currents for different DGs.

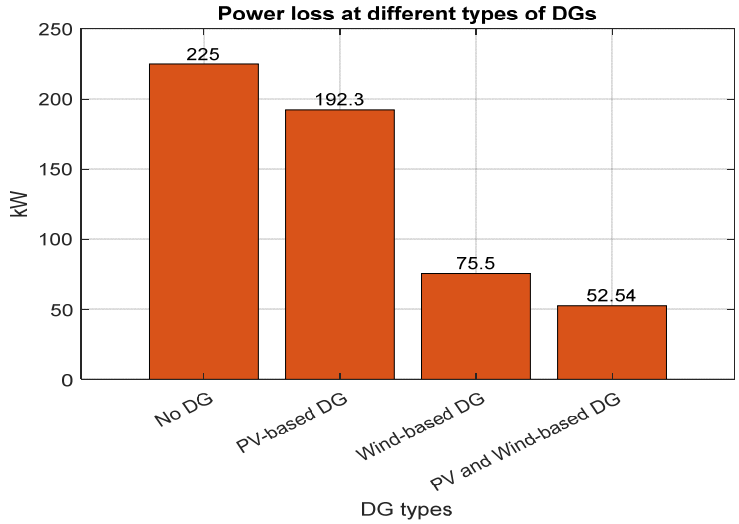

Figure 6. System power losses in different cases.

Lead–acid batteries, lithium-ion batteries, redox flow batteries, and sodium sulfur batteries were chosen as candidate BESSs because they are the most suitable for use in

power distribution and storage systems [18,19]. The power and energy of these BESSs were considered to be available on the market with step sizes of 100 KW/100 kWh, respectively. The candidate buses for the installation of BESSs in the system under study were assumed to include the following: 12, 16, 21, 29, 40, 48, 52, 59, 64, 67, and 69. The comprehensive cost of a BESS encompasses the capital expenditure, power conversion expenses, the balance of the plant cost, construction and commissioning expenditures, fixed operation and maintenance costs, and variable operational costs. Data on the costs and characteristics of BESSs are listed in Table 8.

Table 8. Data on the cost and characteristics of BESSs [31,32].

	Lead–Acid	Lithium Ion	Redox Flow	Sodium Sulfur
Capital Cost—Energy Capacity ($/kWh)	260	271	555	661
Power Conversion System ($/kW)	350	288	350	350
Balance of Plant ($/kW)	100	100	100	100
Construction and Commissioning Cost ($/kWh)	176	101	190	133
Fixed O&M ($/kW-yr)	10	10	10	10
Efficiency	85%	95%	95%	90%
Life Span (yr)	3	10	15	15

4.2. Results and Discussion

Four cases are presented in this study, and each case had five scenarios in which the most economical BESS that has the lowest operation and investment costs and lowest power loss was found. These cases included those with no DGs, a PV-based DG, wind-based DG, and PV and wind-based DGs together. Each case had four scenarios: no BESS, lithium-ion batteries, lead–acid batteries, redox flow batteries, and sodium sulfur batteries, as shown in Table 9. All results will be discussed in detail in the following.

Table 9. The cases and scenarios.

Cases	DG Type	DG Location	Scenarios
1	No DG	--	1. No BESSs 2. Lead–acid 3. Lithium ion 4. Redox flow 5. Sodium sulfur
2	PV	17	1. No BESSs 2. Lead–acid 3. Lithium ion 4. Redox flow 5. Sodium sulfur
3	wind	61	1. No BESSs 2. Lead–acid 3. Lithium ion 4. Redox flow 5. Sodium sulfur
4	PV–wind	61–17	1. No BESSs 2. Lead–acid 3. Lithium ion 4. Redox flow 5. Sodium sulfur

4.2.1. No-DG Case

In this case, it was assumed that the system did not have any DGs, and the impacts of the optimal placement, operation, and sizing of BESSs on the minimization of the investment costs and economic costs of operation of the BESSs were studied. Additionally, we examined the impacts of BESS optimization on system losses and upgrade costs.

In the first scenario, there were no BESSs in the system. The only cost components that were taken into consideration were the system upgrade costs and energy loss costs. In the following four scenarios, BESSs were added to the system, with each having investment and operation costs, as well as system upgrade and energy loss costs. As can be seen in Table 10, it was found that the optimal placement and sizing of the BESSs were at bus #64 and 100 kW, respectively. Each BESS has a different investment cost because BESSs have varying lifespans and different costs on the market. For instance, a lead–acid BESS has the highest NPV investment cost due to its lower lifespan, so it should be replaced many times during a planning period, while a lithium-ion BESS has the lowest investment cost. The economic cost of operation of each BESS is different due to the differences in their efficiency. For instance, lead–acid BESSs boast the highest cost, whereas lithium-ion BESSs have a lower cost than that of lead–acid and sodium sulfur BESSs, and they share the same operational expenses as those of redox flow BESSs due to their identical charging and discharging efficiency. The system upgrade cost was the same in all BESS scenarios, since they had the same placement and sizing. However, it was reduced by 10.45% in comparison with the first scenario due to the deferment of the system upgrade. For instance, feeder #1 was deferred from the third year to the fourth year in this case due to the installation of BESSs. The energy loss cost was slightly reduced by about 0.9% in comparison with that in scenario #1 due to the charging of BESSs during off-peak hours and discharging during on-peak hours. In this case, it was concluded that the lithium-ion BESS had the lowest cost, resulting in savings of 7.04% in comparison with the first scenario. Figure 7 shows the convergence of particle swarm optimization (PSO) in the case in which there were no DGs and in the scenario with lithium-ion batteries.

Table 10. Results for the first case (no DGs).

No DGs	No BESSs	Lead–Acid	Lithium Ion	Redox Flow	Sodium Sulfur
NPV of Investment Cost (M$)	0	0.169	0.095	0.127	0.130
NPV of Economic Cost of Operation (M$)	0	−0.008	−0.0094	−0.0094	−0.0089
NPV of System Upgrade Cost (M$)	3.033	2.716	2.716	2.716	2.716
NPV of Energy Loss (M$)	0.298	0.2954	0.2952	0.2952	0.2953
NPV of Total Cost (M$)	3.3314	3.1712	3.0968	3.1287	3.1323
Saving %	0	4.8	7.04	6.1	5.98
Execution Time (h)			≈1 h		

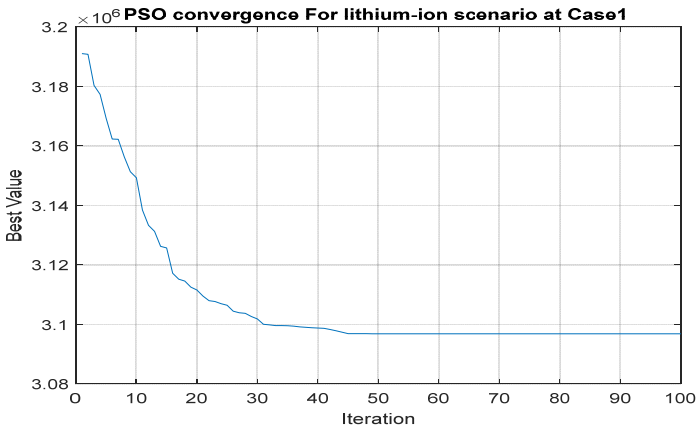

Figure 7. Convergence of PSO in the no-DG case and the lithium-ion scenario.

4.2.2. PV-Based DG Case

In this case, it was previously determined that the PV-based DG was located at bus #17 in order to study its impact on the placement and sizing of BESSs and the impacts of BESS optimization on the economic costs of investment and operation cost, the system cost, and the energy loss cost.

As can be noticed in Table 11, in the 'No BESS' scenario, the system cost remained the same as that in Case #1. This was because the calculation of the system upgrade cost was obtained in the worst-case scenario for the power flow in the network (which was at its maximum in the peak load state and the minimum PV-based state). Nevertheless, there was a 4.36% reduction in energy loss costs due to the installation of the PV-based DG. In the BESS scenario, it was found that the optimal placement and sizing of these BESSs were at bus #64 and 600 kW, respectively. These increases in BESS sizing are attributed to the charging power of the BESSs in the minimum and maximum off-peak load states of the PV-based DG. Each BESS had a different investment cost due to varying lifespans and different costs on the market. In this case, the investment cost significantly increased because of the increase in BESS sizing. For instance, lead–acid batteries incurred an investment cost of $1.011 million, and lithium-ion batteries boasted the lowest investment cost, amounting to just $0.57 million. The economic cost of operation of each BESS varied due to the efficiency of each BESS. In this case, the operation cost significantly increased due to an increase in the power discharge during the peak load state. It was observed that lithium-ion batteries had the lowest operation cost, while lead–acid batteries had the highest cost, since they had the lowest efficiency. The system upgrade cost in the BESS scenarios was the same for all BESS technologies because they shared the same placement and sizing, and their efficiencies were very close to each other. However, it was reduced by 38.3% in comparison with the first scenario due to the deferral of the system upgrade and by 31% in comparison with the first case in the same scenario—for instance, the upgrade decision for feeder #1 was deferred from the third year to the seventh year in the case of BESS inclusion. The energy loss cost experienced significant reductions from the previous case; for example, in the lithium-ion scenario, it was reduced by around 12% in comparison with the first scenario and by about 15.3% in comparison with the first case in the same scenario. It was concluded that the lithium-ion BESS was the most economical choice in this case, with savings of 26.2% in comparison with the first scenario and a 20.85% reduction in costs in comparison with the first case. In contrast, the lead–acid BESS was the least economical BESS option due to its high investment cost, lower efficiency, and shorter lifespan.

Table 11. Results for the second case (PV).

PV-Based DG	No BESS	Lead–Acid	Lithium Ion	Redox Flow	Sodium Sulfur
NPV of Investment Cost (M$)	0	1.011	0.5723	0.764	0.781
NPV of the Economic Cost of Operation (M$)	0	−0.271	−0.243	−0.243	−0.23
NPV of System Upgrade Cost (M$)	3.033	1.872	1.872	1.872	1.872
NPV of Energy Loss (M$)	0.285	0.253	0.2499	0.2499	0.251
NPV of Total Cost (M$)	3.3187	2.9180	2.4512	2.6428	2.6743
Saving %	0	12.1	26.2	20.4	19.4
Execution Time (h)			≈2.5 h		

4.2.3. Wind-Based DG Cases

A. Wind-based DG at 1 MW

In this case, it was previously determined that a 1 MW wind-based DG was located at bus #61 in order to study the impact of a wind-based DG on the placement and sizing of BESSs and the impact of BESS optimization on BESS planning, including the investment cost, operation cost, system cost, and energy loss costs.

Table 12 showcases the NPV of the total planning cost associated with the wind-based DG and BESSs. In the first scenario (no BESSs), the system cost remained the same as that in Case #1 and Case #2, and this was attributed to the calculation of the system upgrade that was obtained in the worst-case scenarios for the power flow in the network, (these occurred in the maximum peak load state and the minimum wind-based state). Nevertheless, there was a 16.1% reduction in the energy loss costs in comparison with Case #1 and a 5.6% reduction in comparison with Case #2. This was due to the installation of the wind-based DG. For the BESS scenarios, it was observed that the optimal placement and sizing for the BESSs were at bus #64 and 1100 kW, respectively. These increases in BESS sizing were attributed to the charging power of the BESSs in the minimum off-peak load state and the maximum state of the wind-based DG. In the following four scenarios, each BESS had a different investment cost because each of them had a different lifespan and different costs on the market. In this case, the investment cost significantly increased due to the increase in BESS sizing. For instance, lead–acid batteries had an investment cost of $1.58 million, and lithium-ion batteries boasted the lowest investment cost, amounting to just $1.05 million.

Table 12. Results for the third case (wind).

Wind-Based DG	No BESS	Lead–Acid	Lithium Ion	Redox Flow	Sodium Sulfur
NPV of Investment Cost (M$)	0	1.85	1.05	1.4	1.43
NPV of Economic Cost of Operation (M$)	0	−0.577	−0.644	−0.644	−0.611
NPV of System Upgrade Cost (M$)	3.033	1.27	1.27	1.27	1.27
NPV of Energy Loss (M$)	0.269	0.1997	0.1954	0.1954	0.1975
NPV of Total Cost (M$)	3.30	2.7426	1.8666	2.2178	2.2857
Saving %	0	16.9	43.4	32.8	30.7
Execution Time (h)				≈3 h	

The economic cost of operation of each BESS varied due to the efficiency of each. In this case, the operation cost significantly increased due to an increase in power discharging during on-peak hours. For instance, the lead–acid battery boasted the highest cost, whereas the lithium-ion battery had a lower cost than that of the lead–acid battery and shared the same operational expenses as those of the redox flow battery due to their identical charging and discharging efficiency. The system upgrade cost in the BESS scenarios was the same for all BESS technologies because they shared the same placement and sizing, and their efficiencies were very close to each other, but it was reduced by 58% in comparison with the first scenario due to the deferral of the system upgrade decision. For instance, feeder #1 was deferred from the third to the tenth year, resulting in a 53.2% reduction in its system upgrade cost in comparison with the first case and a 32.2% reduction in comparison with Case #2 in the same scenarios.

The energy loss cost experienced significant reductions from those in the previous cases; for instance, in the lithium-ion scenario, it decreased by around 27.4% in comparison with the first scenario and by about 33.8% in comparison with the first case, and it decreased by 21.8% in comparison with Case #2 in the same scenarios. It was concluded that the lithium-ion BESS was the most economical choice in this case, with cost savings of 43.4% in comparison with the first scenario, a cost reduction of about 39.8% in comparison with the first case, and a reduction of approximately 23.85% in comparison with Case #2.

Table 13 shows the optimal operation and charging and discharging power of the BESSs in the case of a 1 MW wind-based DG (i.e., in each wind-based DG state and load state); this could help system operators control the operation of BESSs to maximize their benefits for the distribution system. It can be observed in Table 13 that in the initial load state, the charging of the BESSs increased with the increase in the wind state. Conversely, in the final load state, the discharging power of the BESSs decreased with the increase in the wind state. Therefore, the lowest state (i.e., load state = 1 and wind state = 1) had the

lowest charging power. On the other hand, the highest state (i.e., load state = 12 and wind state = 12) had the lowest discharging power.

Table 13. Optimal operation and capacity of BESSs (kW) in the 1 MW wind-based case.

State	Wind State											
	1	**2**	**3**	**4**	**5**	**6**	**7**	**8**	**9**	**10**	**11**	**12**
1	68	118	218	318	418.0004	518.0018	618.002	718.0119	818.0231	918.04	1018.064	1068.078
2	54.38	101.88	196.88	291.88	386.8805	481.882	576.886	671.8937	766.9067	861.9263	956.9537	1004.471
3	40.76	81.16	160.76	240.7601	323.7605	404.1622	484.767	565.7754	646.3901	726.8124	807.8436	848.3628
4	27.14	65.54	142.14	219.1401	295.1405	372.1424	449.143	525.757	602.1735	679.1984	756.2333	794.3749
5	13.52	49.52	122.52	195.5201	282.0206	341.5226	413.528	487.5386	560.1567	633.5842	703.6227	742.6466
6	−0.1	34.9	103.9	169.9001	254.9006	310.9028	379.906	449.9201	518.9398	589.9698	658.012	690.0382
7	−703.72	−671.72	−603.72	−532.72	−463.719	−393.717	−324.711	−268.698	−183.677	−117.645	−48.1989	−13.5705
8	−756.34	−717.34	−647.34	−573.94	−501.339	−427.337	−355.33	−295.817	−209.294	−136.259	−63.7101	−27.1795
9	−807.96	−769.96	−692.96	−615.96	−539.559	−462.957	−385.95	−308.936	−232.911	−155.874	−79.1215	−40.7887
10	−904.58	−821.58	−740.58	−660.18	−579.579	−498.577	−417.569	−337.554	−254.529	−174.489	−94.433	−54.3981
11	−1018.2	−970.7	−918.9	−780.7	−685.699	−2158.2	−495.689	−400.673	−305.646	−210.604	−115.545	−68.0077
12	−1079.5	−1029.5	−929.55	−829.55	−729.549	−629.546	−529.539	−429.522	−329.494	−229.45	−129.388	−79.3492

− indicates the discharging mode.

B. Wind-based DG at 4 MW

In this case, the penetration level of the wind-based DG was increased to 4 MW, which was greater than the rated demand of the system under study. This was to demonstrate how the DG's state 19 controlled the BESSs' status (charging and discharging). In this case, the generated power was greater than the demand, which resulted in excess energy in some scenarios. In order to solve this issue, the system's operator should curtail the excess power from the wind-based DG to reduce its impact on the system's operation (i.e., maintaining the voltages and line currents within their operation limits), and this is not efficient from an economic perspective. Therefore, BESSs can solve this issue due to their ability to absorb excess power. Table 14 shows the optimal operation and charging and discharging power of BESSs in the 4 MW wind-based case (i.e., in each wind-based DG state and load state). Figure 8 illustrates the operation of BESSs and the amounts of charging and discharging power in different selected states of the load and wind (i.e., states #1, 4, 9, and 12 for the load state and wind state) in the 1 MW wind-based DG case and in the 4 MW wind-based DG case. Unlike in the previous case (i.e., the 1 MW wind-based DG), where the charging decisions of the BESSs took place in an off-peak load state and discharging decisions happened in an on-peak load state, the 4 MW wind-based DG case showcased that the BESSs were charged in the maximum wind state (i.e., state #12) regardless of the load state. This was because of the increase in the penetration level of the wind-based DG, which produced excess energy that could be stored by BESSs and used when needed (i.e., the on-load state and off-wind state). Figure 9 shows the voltage profile at each bus in the no-DG, 4 MW wind-based DG, and 4 MW-wind based DG cases with BESSs in the maximum load state and maximum wind state.

Table 14. Optimal operation and capacity of BESSs (kW) in the 4 MW wind-based case.

State	Wind State											
	1	**2**	**3**	**4**	**5**	**6**	**7**	**8**	**9**	**10**	**11**	**12**
1	−1262.7	−862.7	−62.7	737.3	1537.3	1868.002	2268.05	2668.012	2068.023	3468.04	3868.064	4068.078
2	−1466.42	−1066.42	−266.42	533.58	1333.58	1754.382	2184.38	2554.394	2964.407	3350.726	3738.554	4004.471
3	−2050.34	−1656.44	−868.64	−80.8399	706.9605	1640.762	2070.76	2440.775	2808.79	3177.312	3550.844	3918.863
4	−2252.9	−1869.86	−1100.56	−331.56	437.4405	1206.442	1975.45	2317.157	2665.173	3016.698	3367.233	3717.255
5	−2456.5	−2081.93	−1330.23	−578.53	173.1706	924.8726	1676.58	2193.539	2526.057	2861.084	3196.123	3530.647
6	−2660.1	−2294	−1559	−824	−88.9994	646.0028	1381.01	2115.92	2392.44	2711.47	3030.512	3350.038
7	−2865.7	−2505.72	−1786.72	−1067.72	−348.719	370.283	1089.29	1808.302	2153.823	2568.655	2872.501	3176.429
8	−3068.9	−2717.04	−2013.34	−1309.44	−605.639	98.16312	801.97	1505.683	1905.806	2429.241	2718.29	3010.821
9	−3272.7	−2928.16	−2239.16	−1550.16	−861.159	−172.157	516.851	1205.864	1605.889	2301.726	2577.379	2849.211
10	−3476.4	−3138.58	−2462.98	−1787.38	−1111.78	−436.177	239.431	915.0455	1315.071	2266.311	2583.067	2701.602
11	−3680.1	−3348.85	−2686.4	−2023.85	−1361.4	−698.847	−36.3389	625.8267	1025.854	1951.246	2421.955	2556.992
12	−3881.6	−3556.55	−2906.55	−2256.55	−1606.55	−956.546	−306.539	343.4777	743.506	1643.55	2295.612	2420.651

− indicates the discharging mode.

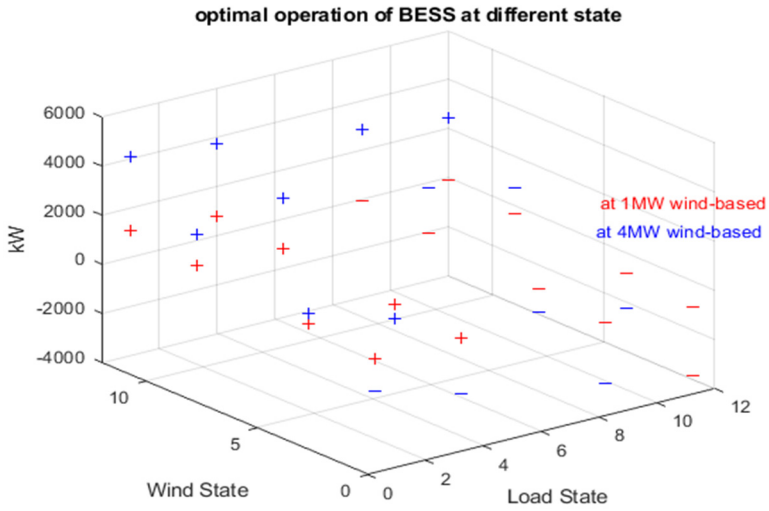

Figure 8. Optimal operation of BESSs in the 1 MW and 4 MW wind-based DG cases in different states. + indicates the charging mode and − indicates the discharging mode.

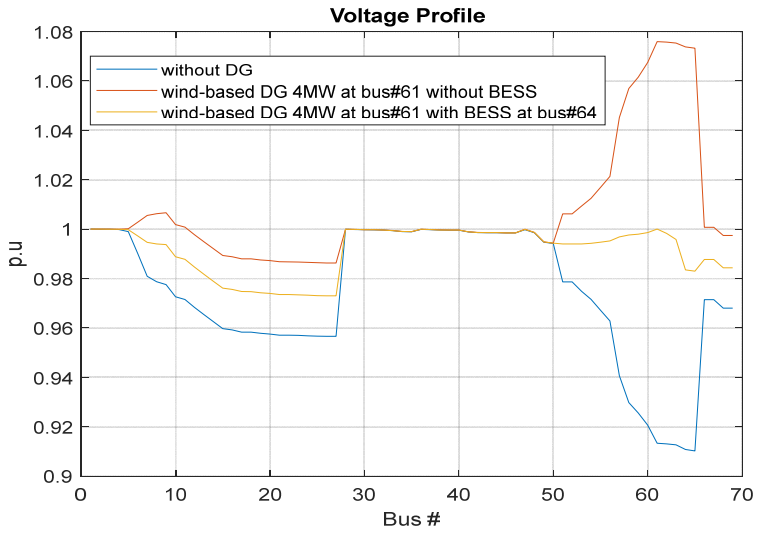

Figure 9. The voltage profile at each bus in the 4 MW wind-based DG case with and without BESSs.

4.2.4. PV and Wind-Based DG Case

In this case, it was determined previously that a 500 kW PV-based DG and a 1 MW wind-based DG were connected to bus #17 and bus #61, respectively, in order to study the common impact of the PV-based DG and wind-based DG on the placement and sizing of BESSs and the impact of BESS optimization on BESS planning, including the BESS investment cost, economic cost of operation, system cost, and energy loss cost.

Table 15 showcases the NPV of the total planning cost associated with the PV and wind-based DGs and BESSs. In the first scenario (no BESSs), the system cost remained the same as that in Cases #1–#3, and this was attributed to the calculation of the system upgrades that was obtained in the worst-case scenarios for the power flow in the network (which occurred in the maximum on-peak load state and the minimum PV and wind-based state). Nevertheless, there was a significant reduction in the energy loss costs in comparison with Case #1, as well as a 14.1% reduction and 10% reduction in comparison with Case #2 and a 4.8% reduction in comparison with Case #3. This reduction was attributed to the installation of PV-based and wind-based DGs together in the system.

Table 15. Results for fourth case (PV and wind).

Wind-Based DG	No BESS	Lead–Acid	Lithium Ion	Redox Flow	Sodium Sulfur
NPV of Investment Cost (M$)	0	2.864	1.622	2.165	2.214
NPV of the Economic Cost of Operation (M$)	0	−0.798	−0.892	−0.892	−0.845
NPV of System Upgrade Cost (M$)	3.033	0.67	0.67	0.67	0.67
NPV of Energy Loss (M$)	0.256	0.185	0.181	0.181	0.183
NPV of Total Cost (M$)	3.2893	2.9212	1.5812	2.1241	2.2221
Saving %	0	11.2	51.9	35.4	32.4
Execution Time (h)			≈8 h		

For the BESS scenario, it became essential to increase the number of BESS units to store a larger amount of energy due to the installation of two DGs with large capacities in the system. Therefore, two BESS units were installed in these cases. It was observed that the optimal placement and sizing of BESS #1 and BESS #2 were at bus #12 and bus #64 with capacities of 600 kW and 1100 kW, respectively. These increases in BESS sizing are attributed to the charging power of the BESSs during the minimum off-peak load state and the maximum output power state of the wind-based and PV-based DGs.

In the following four scenarios, each BESS unit had a different investment cost due to varying lifespans and different costs on the market. In this case, the investment cost significantly increased due to the increase in BESS sizing. Lead–acid batteries had an investment cost of $2.86 million, and lithium-ion batteries boasted the lowest investment cost, amounting to just $1.62 million. The operational cost of each BESS unit varied due to the efficiency of each. In this case, the economic cost of operation significantly increased due to the increase in power charging during the peak load hours. For instance, lead–acid batteries boasted the highest cost, whereas lithium-ion batteries had a lower cost than that of lead–acid batteries and shared the same operational expenses as those of redox flow batteries due to their identical charging and discharging efficiencies.

The system upgrade cost in the BESS scenarios remained the same for all BESS technologies because they shared the same placement and sizing, and their efficiencies were very close to each other. However, the system upgrade cost in the BESS scenario was reduced by 77.9% in comparison with that in the first scenario. This reduction was attributed to the deferral of the system upgrade, as shown in Table 16. For example, feeder #1 was deferred from the 3rd to the 13th year of the planning horizon, and feeders #6, 7, 8, and 9 did not require any upgrades during the planning period. This was due to the installation of BESS units with a large capacity in this case, resulting in a 75% reduction in comparison with the first case, a 64% reduction in comparison with Case #2, and a 47% reduction in comparison with Case #3 in the same scenarios.

Table 16. Years in which distribution feeders were upgraded with and without BESSs in different cases.

State	NO DGs		PV-Based DG		Wind-Based DG		PV- and Wind-Based DGs	
	Upgrade Year without BESSs	Upgrade Year with BESSs	Upgrade Year without BESSs	Upgrade Year with BESSs	Upgrade Year without BESSs	Upgrade Year with BESSs	Upgrade Year without BESSs	Upgrade Year with BESSs
1	3	4	3	7	3	10	3	13
2	3	4	3	7	3	10	3	13
3	3	4	3	7	3	10	3	13
4	5	5	5	9	5	12	5	15
5	3	4	3	8	3	12	3	No upgrade required during planning period
6	3	4	3	8	3	12	3	No upgrade required during planning period
7	3	4	3	9	3	13	3	No upgrade required during planning period
8	4	5	4	9	4	13	4	No upgrade required during planning period
9	5	6	5	10	5	15	5	No upgrade required during planning period

The energy loss cost experienced a significant reduction from those in the previous cases. For example, in the lithium-ion scenario, it decreased by around 29.3% in comparison with the first scenario; it decreased by about 38.7% in comparison with Case #1, by 27.6% in comparison with Case #2, and by 7.4% in comparison with Case #3 in the same scenarios.

In conclusion, the lithium-ion BESS proved to be the most economical choice in this case, with total cost savings of 51.9% in comparison with the first scenario and total cost reductions of about 48.9% in comparison with the first case, about 35.5% in comparison with Case #2, and about 15.3% in comparison with Case #3.

4.3. Sensitivity Analysis

The sensitivity analysis of our proposed model involved varying the key parameters in PSO, such as by exploring different inertia weights (e.g., 0.1, 0.5, 0.9), adjusting the cognitive and social coefficients (e.g., 1.5, 2.0, 2.5), and introducing variations in the initial particle positions. Surprisingly, the results did not exhibit substantial differences when compared with our main PSO configuration with an inertia weight of 0.99 and cognitive and social coefficients of 1.5 and 2, respectively. This suggested that our primary model was robust and displayed a notable insensitivity to parameter variations for the specific optimization task. While these findings affirm the stability of our chosen parameters, future adjustments may be considered based on the requirements of different optimization scenarios.

5. Conclusions

In recent years, numerous innovative technologies such as ESSs and distributed energy resources (DERs) have been seamlessly integrated into distribution networks in response to various technical and economic considerations in order to deliver electricity at the most cost-effective rates while maintaining the necessary level of quality. However, the integration of these ESSs into power systems without thorough research, design, and optimized planning and operational processes could potentially compromise the overall quality and security of electrical grids. Consequently, the optimization of the planning and operation of ESSs is indispensable for bolstering their performance and enhancing the overall quality and reliability of power systems.

The primary objectives of this research were to integrate energy storage systems into distribution systems alongside renewable energy sources and to optimize their placement, operation, and sizing to maximize their benefits while minimizing the total planning and economic costs operation and considering both technical and economic aspects.

This study proposed a probabilistic planning model for BESSs in distribution networks to optimize the location, sizing, and operation of BESSs and to determine the most economically efficient BESS technologies that minimized the overall planning costs. Four different BESS technologies were examined and compared against the base scenario (i.e.,

without BESSs) and each other. It was concluded that the integration of these BESSs into a distribution system in conjunction with a wind-based DG and PV-based DG had a significant impact on reducing energy losses, deferring required system upgrades, and maximizing benefits through energy purchases during off-peak hours and energy selling during on-peak hours. The proposed model demonstrated that lithium-ion battery energy storage was the most cost-effective BESS option for the case under study.

The proposed model proved its effectiveness in accommodating all possible operating scenarios of the system, as well as the intermittent nature of renewable-based DGs. Unlike in previous research work, the proposed model allowed the optimizer to freely make charging and discharging decisions without imposing any unrealistic constraints, leading to more efficient outcomes.

Author Contributions: Conceptualization, A.A.A., M.A.A. and E.A.A.-A.; Funding acquisition, M.A.A.; Investigation, A.A.A., M.A.A. and E.A.A.-A.; Methodology, A.A.A. and M.A.A.; Resources, A.A.A. and M.A.A.; Software, A.A.A.; Supervision, M.A.A. and E.A.A.-A.; Writing—original draft, A.A.A.; Writing—review and editing, M.A.A. and E.A.A.-A. All authors have read and agreed to the published version of the manuscript.

Funding: This research and the APC were funded by K.A.CARE Energy Research and Innovation Center in Riyadh, King Saud University, Riyadh, Saudi Arabia.

Institutional Review Board Statement: Not applicable.

Informed Consent Statement: Not applicable.

Data Availability Statement: The data that support the findings of this study are available from the corresponding author upon reasonable request.

Acknowledgments: The authors extend their appreciation to K.A.CARE Energy Research and Innovation Center in Riyadh, King Saud University, Riyadh, Saudi Arabia for funding this work.

Conflicts of Interest: The authors declare no conflict of interest.

References

1. Farhangi, H. The path of the smart grid. *IEEE Power Energy Mag.* **2010**, *8*, 18–28. [CrossRef]
2. Hossain, E.; Faruque, H.; Sunny, M.; Mohammad, N.; Nawar, N. A Comprehensive Review on Energy Storage Systems: Types, Comparison, Current Scenario, Applications, Barriers, and Potential Solutions, Policies, and Future Prospects. *Energies* **2020**, *13*, 3651. [CrossRef]
3. Hannan, M.; Wali, S.; Ker, P.; Abd Rahman, M.; Mansor, M.; Ramachandaramurthy, V.; Muttaqi, K.; Mahlia, T.; Dong, Z. Battery energy-storage system: A review of technologies, optimization objectives, constraints, approaches, and outstanding issues. *J. Energy Storage* **2021**, *42*, 103023. [CrossRef]
4. Huang, W.-C.; Zhang, Q.; You, F. Impacts of battery energy storage technologies and renewable integration on the energy transition in New York State. *Adv. Appl. Energy* **2023**, *9*, 100126. [CrossRef]
5. Rancilio, G.; Lucas, A.; Kotsakis, E.; Fulli, G.; Merlo, M.; Delfanti, M.; Masera, M. Modeling a large-scale battery energy storage system for power grid application analysis. *Energies* **2019**, *12*, 3312. [CrossRef]
6. Rallabandi, V.; Akeyo, O.M.; Jewell, N.; Ionel, D.M. Incorporating battery energy storage systems into multi-MW grid connected PV systems. *IEEE Trans. Ind. Appl.* **2019**, *55*, 638–647. [CrossRef]
7. Peng, S.; Zhu, L.; Dou, Z.; Liu, D.; Yang, R.; Pecht, M. Method of Site Selection and Capacity Setting for Battery Energy Storage System in Distribution Networks with Renewable Energy Sources. *Energies* **2023**, *16*, 3899. [CrossRef]
8. Das, C.K.; Bass, O.; Kothapalli, G.; Mahmoud, T.S.; Habibi, D. Overview of energy storage systems in distribution networks: Placement, sizing, operation, and power quality. *Renew. Sustain. Energy Rev.* **2018**, *91*, 1205–1230. [CrossRef]
9. Valencia, A.; Hincapie, R.A.; Gallego, R.A. Optimal location, selection, and operation of battery energy storage systems and renewable distributed generation in medium–low voltage distribution networks. *J. Energy Storage* **2021**, *34*, 102158. [CrossRef]
10. Grisales-Noreña, L.F.; Montoya, O.D.; Gil-González, W. Integration of energy storage systems in AC distribution networks: Optimal location, selecting, and operation approach based on genetic algorithms. *J. Energy Storage* **2019**, *25*, 100891. [CrossRef]
11. Johnson, R.C.; Mayfield, M.; Beck, S.B.M. Optimal placement, sizing, and dispatch of multiple BES systems on UK low voltage residential networks. *J. Energy Storage* **2018**, *17*, 272–286. [CrossRef]
12. Wang, B.; Li, H.; Cao, X.; Zhu, X.; Gan, Z. The optimization of energy storage capacity for distribution networks with the consideration of probability correlation between wind farms based on PSO algorithm. *IOP Conf. Ser. Earth Environ. Sci.* **2017**, *61*, 012064. [CrossRef]

13. Saini, P.; Gidwani, L. An investigation for battery energy storage system installation with renewable energy resources in distribution system by considering residential, commercial, and industrial load models. *J. Energy Storage* **2022**, *45*, 103493. [CrossRef]
14. Zhe, J.; Liang, W.; Xuxiang, H.; Xueshan, H.; Dong, Y.; Ning, Z. Distributed Z.: Energy Storage Optimization Configuration of Active Distribution Network. *IOP Conf. Ser. Mater. Sci. Eng.* **2020**, *729*, 012010. [CrossRef]
15. Wang, H.; Wang, J.; Piao, Z.; Meng, X.; Sun, C.; Yuan, G.; Zhu, S. The optimal allocation and operation of an energy storage system with high penetration grid-connected photovoltaic systems. *Sustainability* **2020**, *12*, 6154. [CrossRef]
16. Wong, L.A.; Ramachandaramurthy, V.K.; Walker, S.L.; Taylor, P.; Sanjari, M.J. Optimal placement and sizing of battery energy storage system for losses reduction using whale optimization algorithm. *J. Energy Storage* **2019**, *26*, 100892. [CrossRef]
17. Agamah, S.U.; Ekonomou, L. Energy storage system scheduling for peak demand reduction using evolutionary combinatorial optimization. *Sustain. Energy Technol. Assess.* **2017**, *23*, 73–82.
18. Qiu, J.; Xu, Z.; Zheng, Y.; Wang, D.; Dong, Z. Distributed generation and energy storage system planning for a distribution system operator. *IET Renew. Power Gener.* **2018**, *12*, 1345–1353. [CrossRef]
19. Awad, A.; EL-Fouly, T.; Salama, M. Optimal ESS Allocation for Benefit Maximization in Distribution Networks. *IEEE Trans. Smart Grid* **2017**, *8*, 1668–1678. [CrossRef]
20. Awad, A.; EL-Fouly, T.; Salama, M. Optimal ESS Allocation and Load Shedding for Improving Distribution System Reliability. *IEEE Trans. Smart Grid* **2014**, *5*, 2339–2349. [CrossRef]
21. Leou, R.C. An economic analysis model for the energy storage system applied to a distribution substation. *Int. J. Electr. Power Energy Syst.* **2012**, *34*, 132–137. [CrossRef]
22. Xu, Y.; Singh, C. Adequacy and economy analysis of distribution systems integrated with electric energy storage and renewable energy resources. *IEEE Trans. Power Syst.* **2012**, *27*, 2332–2341. [CrossRef]
23. Alotaibi, A.M.; Salama, M. A multi-state model for renewable resources in distribution systems planning. In Proceedings of the 2014 IEEE Electrical Power and Energy Conference (EPEC), Calgary, AB, Canada, 12–14 November 2014; pp. 48–53.
24. Alotaibi, A.M.; Salama, M. An incentive-based multistage expansion planning model for smart distribution systems. *IEEE Trans. Power Syst.* **2018**, *33*, 5469–5485. [CrossRef]
25. Alotaibi, A.M.; Salama, M. An efficient probabilistic-chronological matching modeling for DG planning and reliability assessment in power distribution systems. *Renew. Energy* **2016**, *99*, 158–169. [CrossRef]
26. Boroumandfar, G.; Khajehzadeh, A.; Eslami, M.; Syah, R.B. Information gap decision theory with risk aversion strategy for robust planning of hybrid photovoltaic/wind/battery storage system in distribution networks considering uncertainty. *Energy* **2023**, *278*, 127778. [CrossRef]
27. Park, J.; Liang, W.; El-Keib, A.A.; Shahidehpour, M.; Billinton, R. A probablistic reliability evaluation of a power system including solar/photovoltaic cell generator. In Proceedings of the 2009 IEEE Power and Energy Society General Meeting, Calgary, AB, Canada, 26–30 July 2009; pp. 1–6.
28. Wong, S.; Bhattacharya, K.; Fuller, J.D. Electric power distribution system design and planning in a deregulated environment. *IET Gener. Transm. Distrib.* **2009**, *3*, 1061–1078. [CrossRef]
29. El-Ela, A.A.A.; El-Sehiemy, R.A.A.; Kinawy, M.; Ali, E.S. Optimal placement and sizing of distributed generation units using different cat swarm optimization algorithms. In Proceedings of the 2016 Eighteenth International Middle East Power Systems Conference (MEPCON), Cairo, Egypt, 7–29 December 2017; pp. 975–981.
30. Pisica, I.; Bulac, C.; Eremia, M. Optimal distributed generation location and sizing using genetic algorithms. In Proceedings of the 15th International Conference on Intelligent System Applications to Power Systems, ISAP, Curitiba, Brazil, 8–12 November 2009; pp. 1–6.
31. Mongird, K.; Viswanathan, V.; Balducci, P.; Alam, J.; Fotedar, V.; Koritarov, V.; Hadjerioua, B. An evaluation of energy storage cost and performance characteristics. *Energies* **2020**, *13*, 3307. [CrossRef]
32. Aquino, T.; Zuelch, C.; Koss, C. *Energy Storage Technology Assessment*; HDR Report No. 10060535-0ZP-C1001; Prepared for the Public Service Company of New Mexico by HDR; HDR: Omaha, NE, USA, 2017.